Supplementary Information

Paper-Based Piezoresistive MEMS Sensors

Xinyu Liu[1], Martin Mwangi[1], XiuJun Li[1], Michael O'Brien[1], and George M. Whitesides[1,2*]

[1] Department of Chemistry and Chemical Biology, [2] Wyss Institute for Biologically Inspired Engineering, Harvard University, Cambridge, MA 02138, U.S.A.

[*]Corresponding author E-mail: gwhitesides@gmwgroup.harvard.edu

Fig. S1 A photograph of the setup for sensor calibration. A paper-based sensor was mounted onto a three-degree-of-freedom (3-DOF) positioner that was used to move the sensor to contact a precision balance. The precision balance was for measuring forces applied to the free end of sensor beam. Resistance changes of the carbon resistor were measured by a LCR (L: inductance, C: capacitance, and R: resistance) meter.

Fig. S1

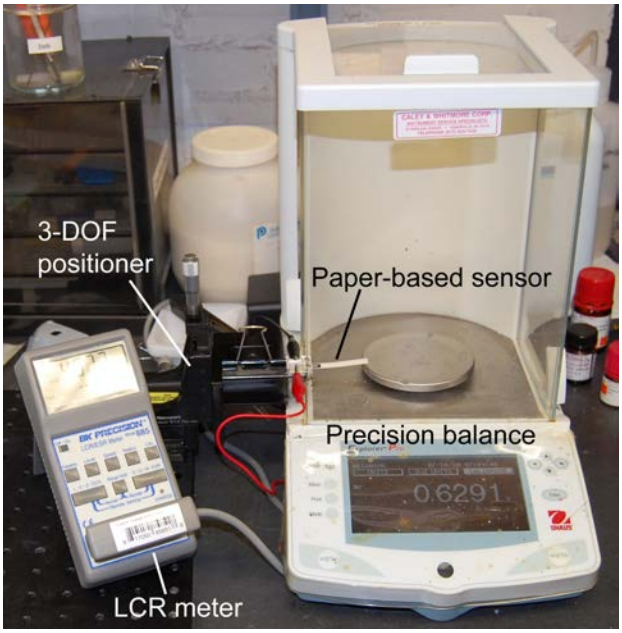
3-DOF
positioner
Paper-based sensor
Precision balance
LCR meter
0.6291

Fig. S2 Mechanical properties of paper cantilever beams. (A) Calibration plots of force-deflection data based on the measurements of 7 devices. The schematic inlets illustrate the types of mechanical strains (stretching vs. compression) applied to the carbon resistors. Error bars represent one standard deviation. The solid line represents a linear fit to the force-deflection data with the regression equation: y = 2.0x (R^2 = 0.9999, N=7). (B) Experimental data of beam stiffness as a function of the number of reciprocating bends. Error bars represent one standard deviation.

Fig. S2

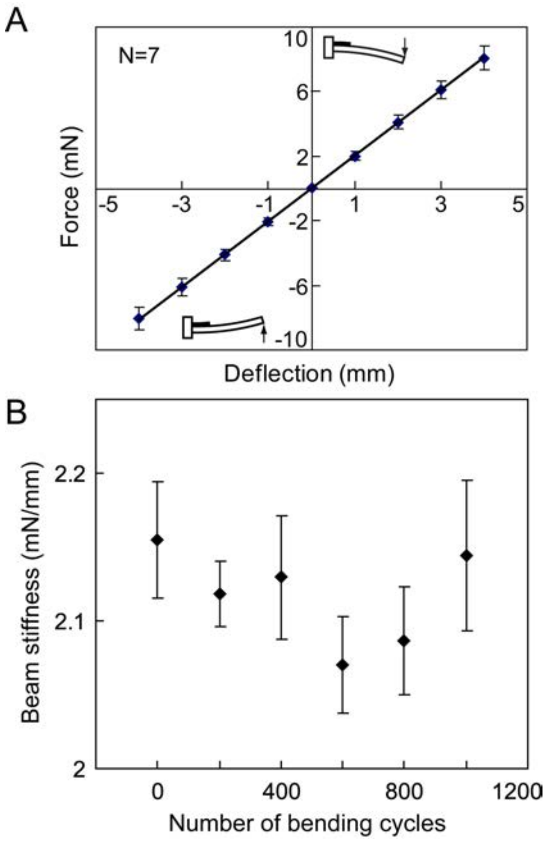
A
N=7
Force (mN)
Deflection (mm)
10
6
2
-2
-6
-10
-5
-3
-1
1
3
5
B
Beam stiffness (mN/mm)
Number of bending cycles
2.2
2.1
2
0
400
800
1200

Fig. S3 Electrical properties of carbon resistors. (A) Linear current-voltage curves for carbon resistors (N=7), showing I-V characteristics of a metal. The slope of a current-voltage curve represents the resistance of the carbon resistor. (B) Calibration plot of the relative change in resistance as a function of the change in temperature. The solid lines represent linear fits to the experimental data with regression equations: y = 0.0006x (blue line, R^2 = 0.92), and y = 0.0005x (brown line, R^2 = 0.91).

Fig. S3

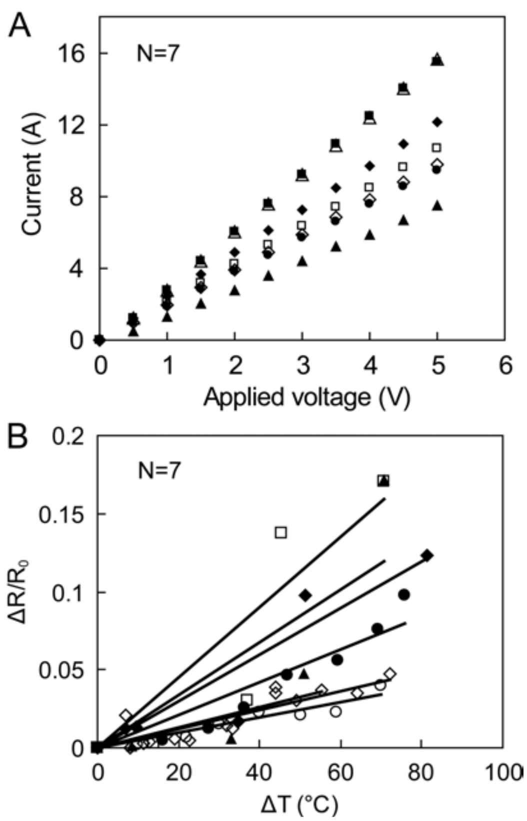

Fig. S4 Sensor calibration data for carbon resistors under stretching strain shows nonlinear behavior. Error bars in all figures represent one standard deviation. (A) Calibration plot of the output (resistance change) of the sensor as a function of the input (applied force), based on measurement of seven devices. The solid line represents a second-order polynomial fit to the experimental data with a regression equation: $y=0.028x^2+0.14x$ ($R^2=0.999$, N=7). (B) Calibration plot of the relative change in resistance as a function of the applied strain. The solid line represents a second-order polynomial fit to the experimental data with a regression equation: $y=3300x^2+2.3x$ ($R^2=0.999$, N=7).

Fig. S4

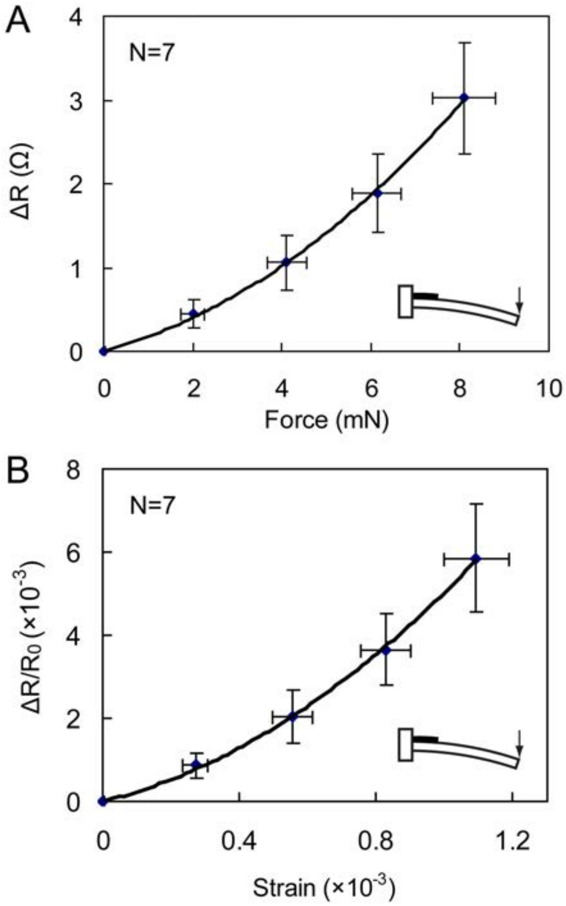
A
N=7
ΔR (Ω)
Force (mN)
0
1
2
3
4
0
2
4
6
8
10
B
N=7
ΔR/R0 (×10-3)
Strain (×10-3)
0
2
4
6
8
0
0.4
0.8
1.2

Fig. S5 Calibration plots of resistance change as a function of applied force based on seven measurements on a sensor: (A) data collected from an un-silanized device, and (B) data collected from a silanized device. These data demonstrate the repeatability of the performance of the sensor. Silanization of the paper surface minimizes the effect of environmental humidity on the performance of the sensor, and the silanized devices produced less variation in output of the sensor than the un-silanized devices. The solid lines represent a linear fit to the experimental data with regression equations: (A) y=0.29x (R^2=0.993, N=seven measurements), and (B) y=0.33x (R^2=0.997, N=seven measurements).

Fig. S5

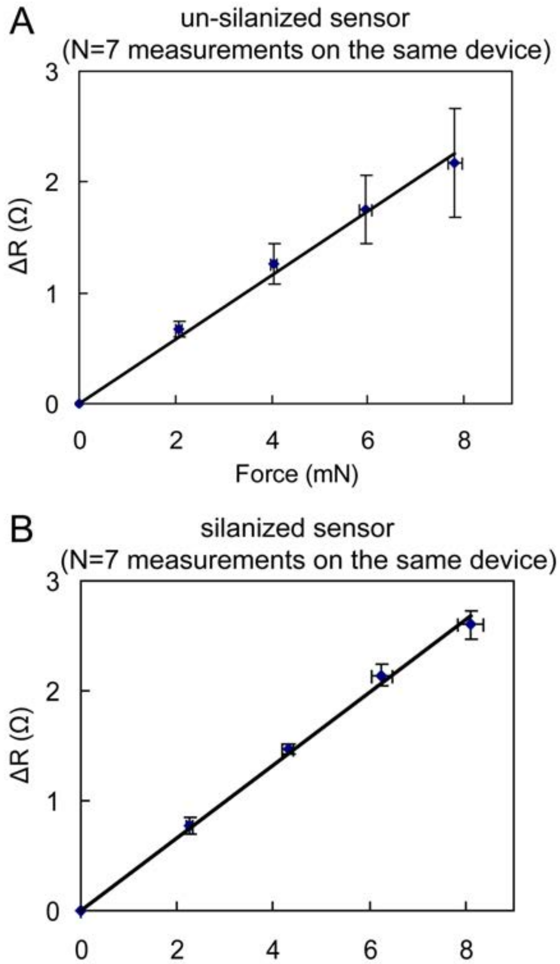
A
un-silanized sensor
(N=7 measurements on the same device)
ΔR (Ω)
0
1
2
3
0
2
4
6
8
Force (mN)
B
silanized sensor
(N=7 measurements on the same device)
ΔR (Ω)
0
1
2
3
0
2
4
6
8

EXPERIMENTAL SECTION

Device fabrication

We patterned the paper cantilever beams by cutting Whatman® 3MM chromatography paper (catalog number: 3030-6185) using a laser cutter (VersaLASER VLS3.50, Universal Laser Systems Inc.). We laid out the carbon resistor and silver contact pad by manually screen-printing graphite ink (or silver ink, for wires) on the paper cantilever.[1] We generated a mask for screen-printing by cutting designed patterns into vinyl stencil film (Grafix® Frisket film) using laser-cutting. We visually aligned the stencil mask with the paper cantilever, placed the mask on top of the cantilever, and filled the openings of the mask with graphite ink (E3456, Ercon) to produce the carbon resistor. We then removed the mask, and dried the paper device on a hotplate at 60 ^{o}C for 20 minutes. After the drying of silver ink, we screen-printed silver ink to form the contact pads following the same procedures.

Dimensions of the PDMS cantilever beams

The dimensions of the PDMS cantilever beams, for characterizing mechanical properties of the cured polymer, are summarized in Table S1. L is length of the beam, and W and H are width and height of the cross-section of the beam respectively.

REFERENCE

1. Z. Nie, F. Deiss, X.Y. Liu, O. Akbulut and G. M. Whitesides, *Lab Chip*, 2010, **10**, 3163-3169.

Table S1 Dimensions of the PDMS cantilever beams for mechanical characterization (in mm).

Mixing ratio (w/w)	Beam	Length (*L*)	Width (*W*)	Height (*H*)
5:1	Beam #1	36.1	9.8	2.3
	Beam #2	40.2	10.4	2.2
	Beam #3	39.2	10.8	2.2
	Beam #4	38.4	10.2	2.3
	Beam #5	39.9	10.1	2.4
	Beam #6	38.6	10.0	2.3
	Beam #7	39.8	11.0	2.2
10:1	Beam #1	41.0	10.3	2.2
	Beam #2	39.7	10.2	2.1
	Beam #3	41.1	9.8	2.2
	Beam #4	40.0	10.1	2.3
	Beam #5	39.8	10.0	2.2
	Beam #6	40.9	10.8	2.3
	Beam #7	40.2	9.9	2.3
20:1	Beam #1	31.3	10.2	2.2
	Beam #2	32.4	9.8	2.1
	Beam #3	32.1	10.1	2.2
	Beam #4	30.4	9.8	2.1
	Beam #5	31.0	10.2	2.2
	Beam #6	32.1	10.1	2.1
	Beam #7	29.7	9.8	2.2